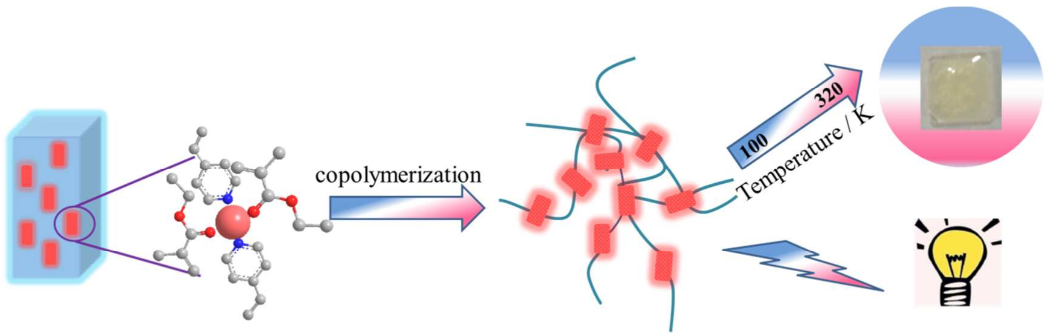

A series of photofunctional polymer hybrid thin films based on rare earth ion-functionalized metal organic frameworks have been synthesized via polymerization reaction. These hybrid polymer thin films are dense and transparent and display multi-colors including blue, red and blue-green. Among which $Y_{0.9}Tb_{0.0999}Eu_{0.0001}$-**2** fabricated hybrid thin film displays white light output. More significantly and interestingly, $Tb_{0.999}Eu_{0.001}$-**2** fabricated hybrid thin film can be used as ratiometric luminescent thermometer based on the energy transfer from Tb^{3+} to Eu^{3+}, whose color will change from blue-green to pink from 100 K to 320 K.

Journal Name RSCPublishing

ARTICLE

Cite this: DOI: 10.1039/x0xx00000x

Received 00th January 2014,
Accepted 00th January 2014

DOI: 10.1039/x0xx00000x

www.rsc.org/

Polymer hybrid thin films based on rare earth ion-functionalized MOF: photoluminescence tuning and sensing as thermometer

Xiang Shen, Bing Yan*

A series of photofunctional polymer hybrid thin films based on rare earth ion functionalized metal organic frameworks (MOFs, **1** for zinc complexes bio-MOF-1 ($Zn_8(ad)_4(BPDC)_6O·2Me_2NH_2$) and **2** for rare earth complexes RE(BPDC)(Ad) (BPDC = biphenyl-4,4'-dicarboxylic acid, Ad = adenine) have been prepared via polymerization reaction of ethyl methacrylate (EMA) and 4-vinylpyridine (VPD). The as-obtained hybrid films are characterized by X-ray diffraction, FT-IR, SEM and especially the luminescence performance and sensing. These hybrid polymer thin films are dense and transparent, which display multi-colors including blue, red and blue-green, respectively. Among which $Y_{0.9}Tb_{0.0999}Eu_{0.0001}$-**2** fabricated hybrid thin film displays white light output. More significantly and interestingly, $Tb_{0.999}Eu_{0.001}$-**2** fabricated hybrid thin film can be used as luminescent ratiometric thermometer based on the energy transfer from Tb^{3+} to Eu^{3+}, whose color will change from blue-green to pink from 100 K to 320 K.

Introduction

Metal complexes, especially porous coordination polymers (PCPs) or metal-organic frameworks (MOFs), are a class of hybrid materials formed by the self-assembly of polydentate bridging ligands and metal-connecting points, which can offer structural diversity and outstanding tenability.[1] MOFs have been growing tremendously over several decades for their various applications, such as drug delivery,[2] gas storage,[3] chemical sensors [4] and so on. In recent years, numerous luminescent MOFs have been reported.[5] There are several ways to generate luminescence in MOFs:[6] direct organic ligands excitation, particularly from the highly conjugated ligands; charge-transfer such as ligand-top-metal charge transfer (LMCT) and metal-to-ligand charge transfer (MLCT); and metal-centered emission, widely exists in rare earth MOFs through the so-called antenna effect[7,8]. Among these, rare earth-doped luminescent MOFs have won a wide range of research interests because rare earth ions have extremely sharp emissions, high color purity and relatively long luminescent lifetimes.[8]

With the increasing practical demand, efforts continue to expand industrial applications and processing path of luminescent MOF. Particularly, the preparation of MOFs as films is a potential domain that has only recently been initiated but which is important for many applications, such as chemical sensors,[9] catalysis,[10] or membranes.[11] More importantly, MOF thin films will show some distinctive and attractive properties for the fabricated luminophores such as rare earth ion or complexes. For instance, the thin films based on rare earth-doped MOFs will show better stability so that they show a broad development prospects [12] and even that there will be a more efficient use of solar energy.[13]

Based on previous research, rare earth-functionalized thin films often come from two closely related fields: zeolite films and coordination polymer films.[14] The most direct approach to produce the former one is to deposit a colloidal suspension on a solid substrate. The colloidal suspension is obtained by embedding zeolite particles into an organic polymer via polymerization reaction.[15] The latter involves Langmuir-Blodgett and layer-by-layer thin film preparation techniques.[16]

Similar to the case of zeolite films, rare earth-doped MOFs can be embedded into organic polymers, which possess the property of flexible coordination ability and obtain novel transparent rare earth polymer thin films via polymerization reaction. To construct this kind of material, polymer unit plays an important role of both as the ligand and host to the doped or central rare earth ions. Organic polymers, including poly(methylmethacrylate),[15a,17] poly(vinylpyridine),[18] poly(ethyleneglycol), are popular candidate for their low optical absorption in the UV region, favorable coordination ability and low synthetic cost.

Herein, we prepare two kinds of photoactive rare earth polymer thin films, which can be expected to have potential application in optical device or chemical sensor. The first kind of polymer film is based on RE-**1** (RE = Eu, Tb) and the second is based on RE-**2** (RE = Y, Eu, Tb). 4-Vinylpyridine and ethyl methacrylate are chosen as the organic polymer units which both coordinate to rare earth ions and occur the copolymerization reaction. All of these hybrid polymer films are characterized and photoluminescence properties are studied. Especially the $Tb_{0.999}Eu_{0.001}$-**2** thin film exhibits luminescent thermometer for the energy transfer from Tb^{3+} to Eu^{3+}.

Experimental section

Chemicals. Chemicals were purchased from commercial sources. All solvent were analytical grade and used without further purification. RE^{3+} nitrates $RE(NO_3)_3{\cdot}xH_2O$ (RE = Y, Eu, Tb) were obtained by dissolving corresponding oxide in nitric acid, followed by evaporation and vacuum drying. $RE(NO_3)_3{\cdot}xH_2O$, adenine, biphenyl-4,4'-dicarboxylic acid (BPDC) and N, N – Dimethylformamide (DMF) were used to synthesize rare earth ions-functionalized coordination polymers. Biphenyl-4,4'-dicarboxylic acid (BPDC, Adamas-beta), 4-vinylpyridine (95 %, VPD, J&K Scientific Ltd.), adenine (Adamas-beta), and ethyl methacrylate (99 %, EMA, Aladdin) were used as received. Ultrapure water and ethanol were used throughout all experiment. Bio-MOF-1 (**1**, $Zn_8(ad)_4(BPDC)_6O{\cdot}2Me_2NH_2$) and rare earth cations encapsulated materials (RE-**1**) were synthesized as described previously.[19]

Synthesis of RE-2 (RE = Eu, Tb; Eu/Tb, Y/Eu/Tb). Ad (0.125 mmol), BPDC (0.125 mmol), $RE(NO_3)_3{\cdot}xH_2O$ (0.125 mmol), DMF (13.5 mL), and water (1 mL) were added to a Teflon-lined autocalve, heated at 150 °C for 24 h, and then cooled to room temperature naturally. The material was collected, washed with DMF (5 mL × 3), and dried under vocuum (24 h). The mixed rare earth materials could be readily synthesized by varying the original molar ratios of $Eu(NO_3)_3{\cdot}xH_2O$ to $Tb(NO_3)_3{\cdot}xH_2O$ (or $Y(NO_3)_3{\cdot}xH_2O$ to $Tb(NO_3)_3{\cdot}xH_2O$ to $Eu(NO_3)_3{\cdot}xH_2O$) through the same synthetic procedures.

Synthesis of Eu-1 polymers hyrids.[15a] A stoichiometric amount of Eu-**1** sample together with a certain amount of 4-vinylpyridine (VPD) was dissolved in 20 mL THF. 0.5 mL of the liquid monomer ethyl methacrylate (EMA) was then introduced into the mixed solution, followed by the initiator benzoyl peroxide (BPO). The amount of BPO was 0.4-0.5 % of the monomer. The final mixture is continued to be agitated for approximately 12 h at 80 °C to obtain the polymers thin film. Other hybrid thin films, PEMA-PVPD-Tb-**1**, and PEMA-PVPD-RE-**2** (RE = E, Tb, Eu/Tb, Y/Eu/Tb) were prepared in the same way.

Preparation of thin films. All the rare earth polymer thin films were prepared by a direct spin-coating method through dripping the prepared colloid sample dissolved in an appropriate amount of THF onto a pre-cleaned 2 cm × 2 cm glass. Polymer hybrids were dripped onto a 1.0 cm × 1.0 cm quartz glass. The solvent was removed by drying the thin film at room temperature.

Physical characterization. X-ray powder diffraction patterns (XRD) were collected using a Bruker Foucs D8 at 40kV, 40mA for Cu-Kα with a scan speed of 0.10 sec/step and a step size of 0.02 °; the data were collected within 2θ range of 3-50 °. Scanning electronic microscope (SEM) images were obtained with a Hitachi S-4800. Fourier transform infrared spectra (FTIR) were measured with KBr slices from 4000 to 400 cm^{-1} using a Nexus 912AO446 infrared spectrum radiometer.

Luminescent measurements. The luminescence spectra were recorded on an Edinburgh FL920 phosphorimeter using a 450 W xenon lamp as excitation source as well as the luminescence lifetime. The quantitative value of lifetime is calculated by linear fitting. The outer luminescent quantum efficiency was determined using an integrating sphere from Edinburgh FLS920 phosphorimeter.

Sensing.[20] $Tb_{0.999}Eu_{0.001}$-**2** polymer thin film was detected for sensing of temperature. The mixed coordination polymer thin film was used to detect the changing luminescence intensity based on different temperatures.

Results and discussion

Two series of materials both based on adenine (Ad) and biphenyl-4,4'-dicarboxylic acid (BPDC) organic ligands are hydrothermally synthesized with different central metal ions, zinc ions and ytterbium ions respectively. **1** is chosen because it has a rigid permanently porous structure for hosting and sensitizing rare earth cations and it is an anionic MOF so that rare earth ions can easily enter into the MOF via straightforward cation exchange experiments and the structure of the framework retains.[19,21] Therefore, in Figure S1a, The X-ray diffraction patterns show that the powder materials still retain their crystallinity after loading rare earth ions of Eu^{3+} and Tb^{3+}. Based on this, another series of rare earth complexes, RE-**2** (RE = Y, Eu, Tb) are further synthesized by the reaction of adenine and BPDC with $Ln(NO_3)_3$ at 150 °C for 24 h. In Figure S1b, the XRD patterns show the structure of this series of RE-**2** powder materials are isostructural. After powder samples synthesized successfully, the as-prepared thin films using glass as the substrate can be roughly depicted in Scheme 1. 4-Vinylpyridine (VPD) and ethyl methacrylate (EMA) are chosen as organic polymer units for that the N atom in pyridine ring of VPD and the O atom of carbonyl group can coordinate with rare earth ions. In the circumstance of initiator and certain temperature, both of them could react with each other through polymerization reaction. Finally, thin films are obtained by depositing colloidal suspension on a solid substrate.

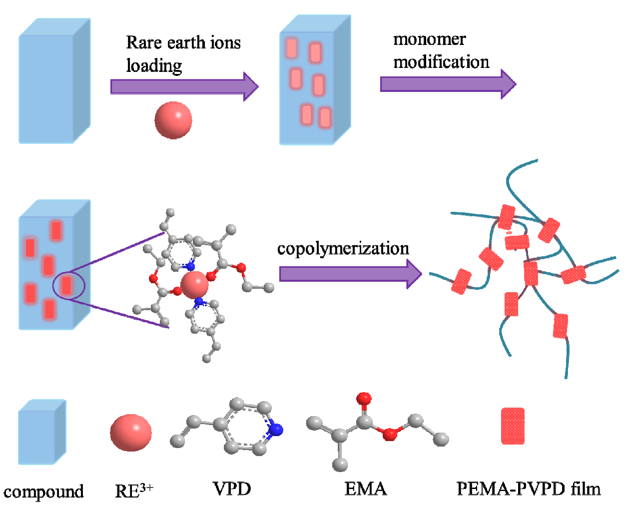

Scheme 1 Procedure for obtaining luminescent rare earth polymer thin films: polymers including EMA and VPD coordinate with the rare earth ions loaded

into the substrate and then both of them can react via polymerization reaction in the circumstance of initiator.

The FT-IR spectra of powder (Line b) and thin film (Line a) samples of Y-**2** are shown in Figure 1 and the corresponding IR spectrum of **1** is shown in Figure S2. Compared with Line b, Line a shows two strong absorption bands at 2984 cm^{-1} and 1727 cm^{-1} respectively. The wavenumber of 2984 cm^{-1} belongs to -CH_2- stretching vibrations after the polymerization reaction between VPD and EMA while the wavenumber of 1727 cm^{-1} belongs to C=O stretching vibrations in EMA.[22] Besides, the absorption band at 1600 cm^{-1} and 1417 cm^{-1} can also be observed, which represent benzene ring stretching vibrations of BPDC and C4N9 stretching vibrations of adenine respectively (Figure S11).[23] Conclusively, the powder of Y-**2** has successfully and effectively reacted with VPD and EMA via polymerization reaction. The same result can also be observed in RE-**1** film as well (Figure S2). Both -CH_2- stretching vibrations (2986 cm^{-1}) and C=O stretching vibrations (1729 cm^{-1}) can be found on the basis that the structure retains after the polymerization reactions.

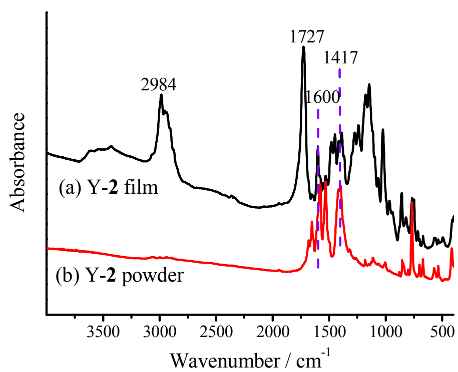

Figure 1 FT-IR spectra of Y-**2** thin film (a) and powder (b).

The scanning electron microscopy (SEM) image of Y-**2** polymer thin film is shown in Figure 2a. The film surface is smooth, continuous and defect-free over a large area. It is noted that the thin film is transparent in the photograph (Figure 2b).

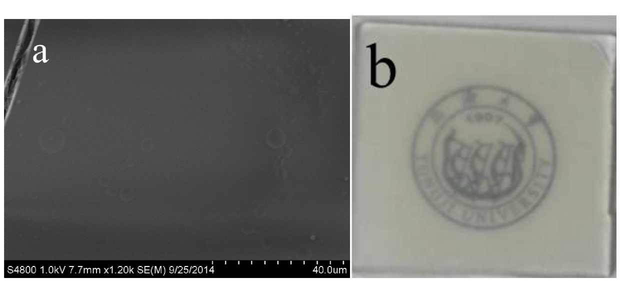

Figure 2 Selected SEM image of Y-**2** thin film (a) viewed from surface and the photograph of the transparent thin film (b).

Figure 3 shows the luminescent spectra of Y-**2** and **1** thin films. Without loading rare earth ions into the framework, the emission of Y-**2** film is located in blue bands when excited at 371 nm and its excitation spectrum is obtained by monitoring the emission wavelength at 445 nm, whose colour is blue. Accordingly, pure **1** film exhibits a blue light when excited at 351 nm. Compared with powder samples in Figure S4, both of them display red shifts in their emission spectra. We suppose that these changes are due to the copolymers of PEMA-PVPD. To prove the point, the excitation and emission spectra of PEMA and PVPD are detected in Figure S3. A broad band ranging from 420 to 500 nm in the emission spectrum can be observed when excited at 378 nm and the excitation spectrum is obtained by monitoring the wavelength at 480 nm. In result, with the different amount of polymer compounds in thin films, they exhibit red shifts in their emission spectra.

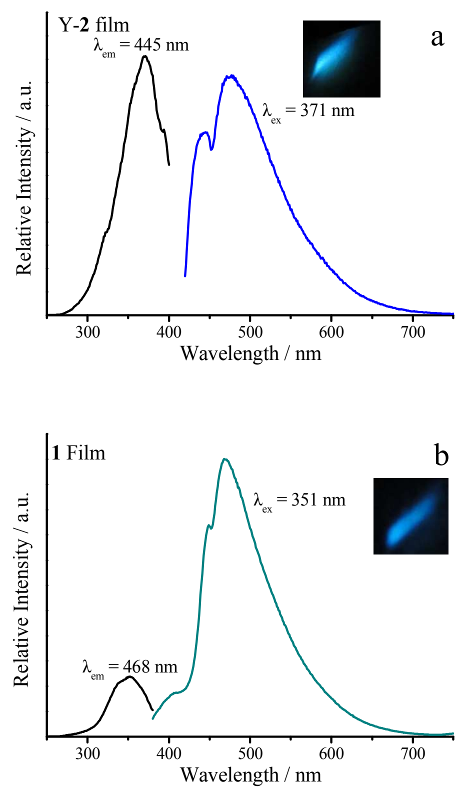

Figure 3 The excitation (black) and emission (blue) spectra of Y-**2** thin film (a) (λ_{ex} = 371 nm, λ_{em} = 445 nm) and **1** thin film (b) (λ_{ex} = 351 nm, λ_{em} = 468 nm), the insets shows each luminescent photograph of (a) and (b) under xenon lamp which colours are both blue.

The excitation and emission spectra of two kinds of Eu^{3+} ions functionalized materials are shown in Figure 4 and the corresponding luminescent spectra of powders are shown in Figure S5. Both materials are measured at room temperature. The emission of Eu-**2** powder exhibits the Eu^{3+} characteristic transitions at 579, 593, 614, 652 and 700 nm under the excitation at 321 nm, which are ascribed to the $^5D_0 \rightarrow {}^7F_J$ (J = 0-4) transitions. The excitation spectrum is obtained by monitoring the emission wavelength at 614 nm, which is dominated by a broad band centered at about 321 nm and two sharp lines, assigned to the $^7F_0 \rightarrow {}^5L_6$ (at 394 nm) and $^7F_0 \rightarrow {}^5D_2$ (at 463 nm) (Figure S5a). Generally, the excitation wavelength of trivalent rare earth ions greatly depends on the ligands, which is so called "antenna effect".[7,8] Figure 4a shows the excitation and emission spectra of its thin film. The characteristic emission of Eu^{3+} can be observed as well when excited at 322 nm. The excitation spectrum is obtained by monitoring the emission wavelength at 614 nm. In addition, the luminescent spectrum of another kind of Eu-**1** polymer thin film is shown in Figure 4b and the corresponding luminescent spectrum of powder sample is shown in Figure S5b. The characteristic transition of Eu^{3+} can be observed under the excitation at 317 nm. The excitation spectrum is obtained by monitoring the wavelength at 616 nm. Unlike the emission spectrum of powder sample (Figure S5b), the typical intra-configurational transitions of Eu^{3+} ions exhibit very week intensity in the excitation spectra illustrating an efficient energy transfer from the organic ligands to Eu^{3+} ions. Insets in Figure 4a and 4b are luminescent photographs of these films under xenon lamp. The red colour in Figure 4a is much stronger than that in Figure 4b, which may be caused by the following two reasons. One is that in terms of structure, Eu^{3+} ions are loaded in the cage of **1** via cations exchange while those of Eu-**2** exist in the framework stably; the other is that in terms of the luminescent emission spectra, the emission intensity of Eu^{3+} in Figure 4a is much stronger than that in Figure 4b. Therefore, Eu-**2** thin film shows bright red colour while Eu-**1** thin film shows dark red colour. The white spots in Figure 4a inset is reflection from the light source which can't be found in Figure 4b inset in that the photograph is taken under the situation of avoiding light reflection.

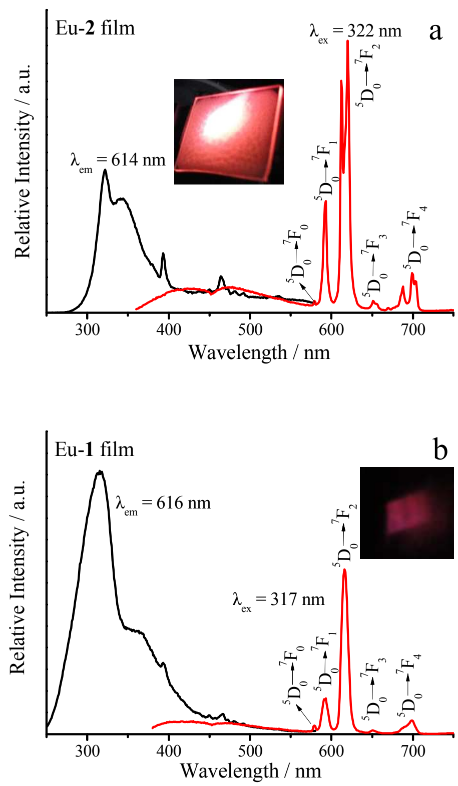

Figure 4 The excitation (black) and emission (red) spectra of Eu-**2** (a) (λ_{ex} = 322 nm, λ_{em} = 614 nm) and Eu-**1** (b) (λ_{ex} = 317 nm, λ_{em} = 616 nm) thin films and their luminescent photographs show red colours under xenon lamp.

Two kinds of Tb^{3+} ions doped materials have been researched as well. The excitation and emission spectra of two samples are shown in Figure 5 and that of powder samples are shown in Figure S6. Figure 5a shows the luminescent properties of Tb-**2** polymer thin film. The emission exhibits the Tb^{3+} characteristic transitions at 490, 545, 587 and 622 nm under the excitation at 321 nm, which are ascribed to the $^5D_4 \rightarrow {}^7F_J$ (J = 6-3) transitions. The characteristic transition of Tb^{3+} can be observed as well in the sample of Tb-**1** when excited at 317 nm in Figure 5b. The excitation spectra are obtained by monitoring the emission wavelength at 545 nm. Furthermore, compared with the powder (Figure S6), except the characteristic transitions of Tb^{3+} ions, a broad band centred from 400 to 480 nm can be observed, which is caused by the luminescence of polymer compounds, PEMA and PVPD. Insets in Figure 5a and Figure 5b are photographs of Tb^{3+} doped polymer thin films under xenon lamp. Both of them display blue-green colours.

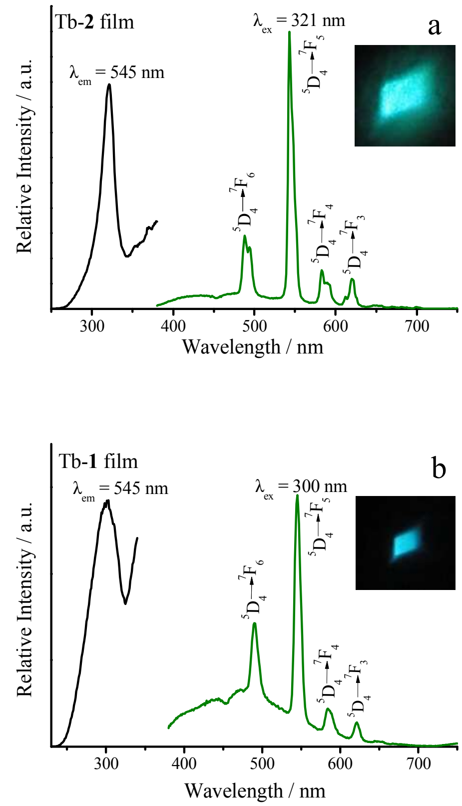

Figure 5 The excitation (black) and emission (green) spectra of Tb-**2** thin film (a) (λ_{ex} = 321 nm, λ_{em} = 545 nm) and Tb-**1** thin film (b) (λ_{ex} = 300 nm, λ_{em} = 545 nm) and the photographs display blue-green.

Further, $Y_{0.9}Tb_{0.0999}Eu_{0.0001}$-**2**, a mixed rare earth material, was synthesized and prepared as a thin film via a direct spin-coating method. Figure S7 displays the excitation and emission spectra of the corresponding powder sample. The characteristic emission of Tb^{3+} at 545 nm and that of Eu^{3+} at 614 nm can be observed simultaneously, when excited at 335 nm. The excitation spectrum is obtained by monitoring the wavelength of 614 nm. The inset in Figure S7 is its CIE chromaticity diagram showing the sample's colour is pink. The luminescent spectrum of film is displayed in Figure 6, which is not only shows the characteristic transition ($^5D_4 \rightarrow {}^7F_5$) of Tb^{3+} but also shows the characteristic transition ($^5D_0 \rightarrow {}^7F_2$) of Eu^{3+} when excited at 329 nm. Different from the powder (Figure S7), a broad band from 400 to 500 nm in the emission spectra is caused by the luminescence of polymer compounds. More importantly, this kind of thin film displays white light output (x = 0.3, y = 0.2951, Figure S8) at the excitation of 329 nm (Figure 6 inset) which shows a great potential and significant applications in optical and electronic devices in the future.

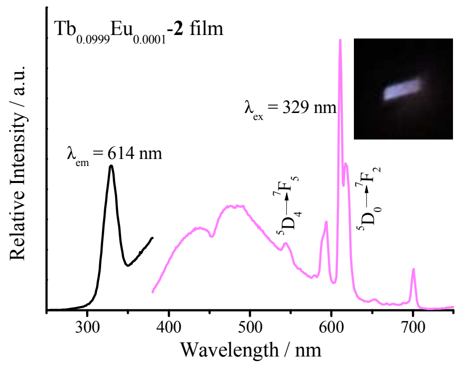

Figure 6 The excitation (black) and emission (pink) spectra of $Tb_{0.0999}Eu_{0.0001}$-**2** thin film (λ_{ex} = 329 nm, λ_{em} = 614 nm) and the inset is the photoluminescence colour exhibiting white.

Based on the above phenomenon that the emission intensity of Eu^{3+} is much higher than Tb^{3+} in the mixed rare earth polymer thin film while the amount of Eu^{3+} is slight, we suppose that the emission of Eu^{3+} ions can further sensitized by the Tb^{3+} ions, that is, there exists energy transfer from Tb^{3+} to Eu^{3+}. According to this, another terbium and europium mixed complex, $Tb_{0.999}Eu_{0.001}$-**2** thin film, was synthesized. Figure S9 shows its excitation and emission spectra. The characteristic emissions of Tb^{3+} at 545 nm and Eu^{3+} at 614 nm exist simultaneously and the emission intensity of Eu^{3+} is four times higher than that of Tb^{3+}. In addition, lifetimes of relevant samples are detected likewise. The lifetimes of Eu-**2** film and Tb-**2** film are 1229.37 μs and 385.49 μs respectively. Compared with lifetimes of the above, the Eu^{3+} lifetime in the mixed material rises to 1322.41 μs while Tb^{3+} lifetime is decreased to 269.81 μs, which proves the energy achievement of Tb^{3+}. (See Table S1) Based on the change of lifetimes, the potential of $Tb_{0.999}Eu_{0.001}$-**2** thin film acted as a luminescent thermometer is explored. Especially, the substrate has been changed to quartz glass instead of ordinary glass, which has no emission under UV excitation. As a result, no luminescence of substrate can be found during the whole process of temperature changing.

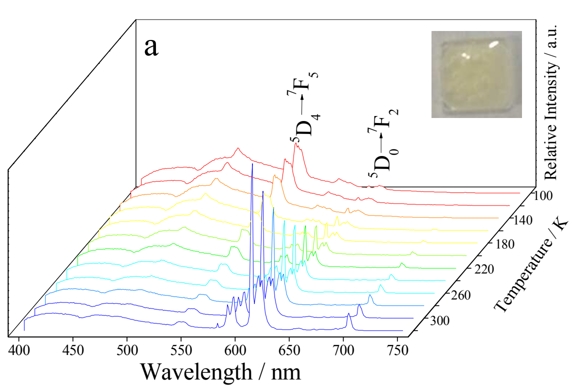

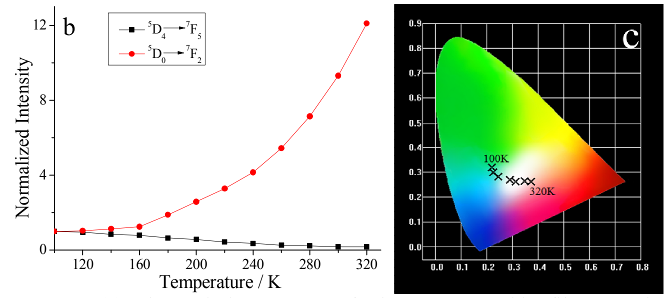

Figure 7 (a) The emission spectra of $Tb_{0.999}Eu_{0.001}$-**2** thin film recorded ranging from 100 K to 320 K excited at 329 nm, (b) temperature-dependent intensity of the $^5D_4\rightarrow{}^7F_5$ and $^5D_0\rightarrow{}^7F_2$ transition, (c) CIE chromaticity diagram showing the luminescence colors changing from blue-green to pink cross white area at different temperatures.

The temperature-dependent photoluminescent (PL) properties of this thin film are investigated in terms of intensity in order to establish their potentials as luminescent thermometer.[24] The temperature dependence of the emission spectra from 100 K to 320 K is illustrated in Figure 7a, and the integrated intensities of the $^5D_4\rightarrow{}^7F_5$ (Tb^{3+}, 545 nm) and $^5D_0\rightarrow{}^7F_2$ (Eu^{3+}, 616 nm) transitions are shown in Figure 7b. The emission intensity of Tb^{3+} ions decreases, while that of Eu^{3+} ions increases with the temperature changing from 100 K to 320 K. In Figure 7a, the emission bands of 614 nm (Eu^{3+}) is much weaker than that of 545 nm (Tb^{3+}) at 100 K because the energy transfer hasn't occurred in the low temperature. Whereas at 320 K, the emission of Eu^{3+} almost dominates the whole spectrum and the emission of Tb^{3+} nearly disappears although the Eu^{3+} content is very low. That is to say, with the temperature rising, the energy transfer from Tb^{3+} to Eu^{3+} occurs and the phenomenon is very effective and remarkable. The inset in Figure 7a is the photograph of the thin film which is fabricated in a 1 cm×1 cm quartz glass by spin coating and displays transparent. Figure 7b shows visually the change of $^5D_4\rightarrow{}^7F_5$ (Tb^{3+}, 545 nm) and $^5D_0\rightarrow{}^7F_2$ (Eu^{3+}, 616 nm) transitions. With the temperature changing from 100 K to 320 K, the normalized intensity of Tb^{3+} decreases gradually while that of Eu^{3+} ascent in a graceful curve. The temperature-dependent luminescence color is tuned from the blue-green to pink cross the white light area from 100 K to 320 K, systematically. Based on CIE chromaticity diagram, the corresponding CIE coordinates change from (0.2194, 0.3198) at 100 K to (0.3719, 0.2657) at 320 K.

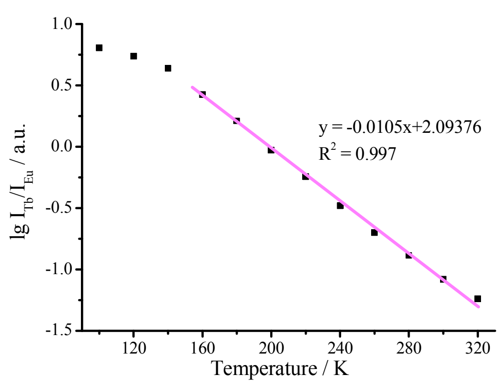

Figure 8 The fitted curve for $Tb_{0.999}Eu_{0.001}$-**2** polymer thin film at the range of 150-320 K

The different temperature-dependent luminescent emissions of $^5D_4\rightarrow^7F_5$ (Tb^{3+}, 545 nm) and $^5D_0\rightarrow^7F_2$ (Eu^{3+}, 616 nm) have enabled this film to be excellent candidates for self-referencing luminescent thermometers. Because the energy transfer between Tb^{3+} and Eu^{3+} is very evident and efficient, the original intensity ratio I_{Tb}/I_{Eu} decreases with an exponential function (Figure S10). The absolute temperature measurement can be linearly correlated to $lg(I_{Tb}/I_{Eu})$ from 160 K to 320 K , and the thermal sensitivity is 1.05 %°C^{-1}(Figure 8). Table S1 shows the luminescent data of these hybrid thin films. The absolute luminescent quantum efficiency η is an important parameter in the evaluation of the efficiency of the emission process in luminescent materials. All the hybrid polymer films possess high quantum efficiencies, which reveals the good luminescence properties of these materials.

Conclusions

In summary, two series of rare earth polymer thin films via coordinating with organic polymer ligands, 4-vinylpyridine (VPD) and ethyl methacrylate (EMA) through polymerization reaction. All of these hybrid materials are dense and transparent. Under excitation of different wavelength, these polymer thin films can emit multi-color visible luminescence depending on the different rare earth ions, including blue, red and blue-green color. Furthermore, the mixed polymer thin film doped with Eu^{3+} and Tb^{3+} displays white light under the excitation of 329 nm, which can be applied to optic devices. Most promisingly, $Tb_{0.999}Eu_{0.001}$-**2** polymer thin film can act as a luminescent thermometer because the color changes distinctly from 100 K to 320 K and its range of temperature response is wide as well.

Acknowledgements

This work was supported by the National Natural Science Foundation of China (91122003) and the Developing Science Funds of Tongji University.

Notes and references

Department of Chemistry, Tongji University, Shanghai 200092, P. R. China. Tel: (+86) 21-65984663; E-mail: byan@tongji.edu.cn

† Electronic Supplementary Information (ESI) available: Experimental, synthesis and characterization details. See DOI: 10.1039/b000000x/

1. H. C. Zhou, J. R. Long and O. M. Yaghi, *Chem. Rev.*, 2012, **112**, 673.
2. (*a*) X. Y. Zhu, J. L. Gu, Y. Wang, B. Li, Y. S. Li, W. R. Zhao and J. L. Shi, *Chem. Commun.*, 2014, **50**, 8779; (*b*) Q. Hu, J. C. Yu, M. Liu, A. P. Liu, Z. S. Dou and Y. Yang, *J. Med. Chem.*, 2014, **57**, 5679; (*c*) J. S. Qin, D.-Y. Du, W. L. Li, J.-P. Zhang, S.-L. Li, Z. M. Su, X.-L. Wang, Q. Xu, K. Z. Shao and Y. Q. Lan, *Chem. Sci.*, 2012, **3**, 2114.
3. (*a*) J. Sim, H. Yim, N. Ko, S. B. Choi, Y. Oh, H. J. Park, S. Park and J. Kim, *Dalton Trans.*, 2014, DOI:10.1039/C4DT02300E; (*b*) Z. X. Wang, B. S. Zheng, H. T. Liu, X. Lin, X. Y. Yu, P. G. Yi and R. R. Yun, *Cryst. Growth. Des.*, 2013, **13**, 5001; (*c*) Y. S. Xue, Y. He, S. B. Ren, Y. Yue, L. Zhou, Y. Z. Li, H.-B. Du, X. Z. You and B. Chen, *J. Mater. Chem.*, 2012, **22**, 10195.
4. (*a*) C. B. He, K. D. Lu and W. B. Lin, *J. Am. Chem. Soc.*, 2014, **136**, 12253; (*b*) Y. Lu and B. Yan, *Chem. Commun.*, 2014, **50**, 15443; (*c*) Y. Zhou, H.-H. Chen and B. Yan, *J. Mater. Chem. A*, 2014, **2**, 13691.
5. (*a*) P. Falcaro, R. Ricco, C. M. Doherty, K. Liang, A. J. Hill and M. J. Styles, *Chem. Soc. Rev.*, 2014, **43**, 5513; (*b*) Y. Zhou and B. Yan, *Inorg. Chem.*, 2014, **53**, 3456; (*c*) Z.-F. Liu, M. F. Wu, S.-H. Wang, F.-K. Zheng, G. E. Wang, J. Chen, Y. Xiao, A. Q. Wu, G. C. Guo and J.-S. Huang, *J. Mater. Chem. C*, 2013, **1**, 4634; (*d*) Y. A. Li, S.-K. Ren, Q.-K. Liu, J. P. Ma, X. Chen, H. Zhu and Y. B. Dong, *Inorg. Chem.*, 2012, **51**, 9629; (*e*) T. W. Duan and B. Yan, *J. Mater. Chem. C*, 2014, **2**, 5098.
6. (*a*) M. D. Allendorf, C. A. Bauer, R. K. Bhakta and R. J. T. Houk, *Chem. Soc. Rev.*, 2009, **38**, 1330; (*b*) Y. J. Cui, Y. F. Yue, G. D. Qian and B. L. Chen, *Chem. Rev.*, 2012, **112**, 1126.
7. (*a*) Binnemans, K. *Chem. Rev.* 2009, **109**, 4283; (*b*) Sabbatini, N.; Guardigli, M.; Lehn, J.-M. *Coord. Chem. Rev.*1993, **123**, 201; (*c*) Moore, E. G.; Samuel, A. P. S.; Raymond, K. N. Acc. *Chem. Res.* 2009, **42**, 542.
8. (*a*) B. Yan, *RSC. Adv.*, 2012, **2**, 9304; (*b*) L. D. Carlos, R. A. S. Ferreira, V. D. Bermudez and S. J. L. Ribeiro, *Adv. Mater.*, 2009, **21**, 509; (*c*) J. Feng and H. J. Zhang, *Chem. Soc. Rev.*, 2013, **42**, 387.
9. (*a*) P. A. Szilagyi, R. J. Westerwaal, R. van de Krol, H. Geerlings and B. Dam, *J. Mater. Chem. C*, 2013, **1**, 8146; (*b*) H. Liu, H. Wang, T. Chu, M. Yu and Y. Yang, *J. Mater. Chem. C*, 2014, **2**, 8683; (*c*) Y. M. Zhu, C.-H. Zeng, T. S. Chu, H. M. Wang, Y. Y. Yang, Y. X. Tong, C. Y. Su and W. T. Wong, *J. Mater.Chem. A*, 2013, **1**, 11312.
10. W. Zhang, G. Lu, S. Li, Y. Liu, H. Xu, C. Cui, W. Yan, Y. Yang and F. Huo, *Chem. Commun.*, 2014, **50**, 4296.
11. J. Gascon and F. Kapteijn, *Angew. Chem. Int. Edit.*, 2010, **49**, 1530.
12. (*a*) Y. Lu and B. Yan, *J. Mater. Chem. C*, 2014, **2**, 5526; (*b*) Y. Zhang and J. H. Hao, *J. Mater. Chem. C*, 2013, **1**, 5607.
13. K. Binnemans, *Chem. Rev.*, 2009, **109**, 4283.
14. (*a*) A. Bétard and R. A. Fischer, *Chem. Rev.*, 2011, **112**, 1055; (*b*) O. Shekhah, J. Liu, R. A. Fischer and C. Woll, *Chem. Soc. Rev.*, 2011, **40**, 1081.
15. (*a*) H. Li, Y. Ding, P. Cao, H. Liu and Y. Zheng, *J. Mater. Chem.*, 2012, **22**, 4056; (*b*) X. F. Qiao and B. Yan, *Inorg. Chem.*, 2009, **48**, 4714; (*c*) J.-N. Hao and B. Yan, *New J.Chem.*, 2014, **38**, 3540.
16. R. Makiura, S. Motoyama, Y. Umemura, H. Yamanaka, O. Sakata and H. Kitagawa, *Nat. Mater.*, 2010, **9**, 565.
17. H. F. Jiu, J. J. Ding, Y. Y. Sun, J. Bao, C. Gao and Q. J. Zhang, *J. Non-Cryst. Solids.*, 2006, **352**, 197.
18. X. F. Qiao and B. Yan, *J. Phys. Chem. B*, 2008, **112**, 14742.
19. J. Y. An, S. J. Geib and N. L. Rosi, *J. Am. Chem. Soc.*, 2009, **131**, 8376.
20. (*a*) Y. J. Cui, H. Xu, Y. F. Yue, Z. Y. Guo, J. C. Yu, Z. X. Chen, J. K. Gao, Y. Yang, G. D. Qian and B. L. Chen, *J. Am. Chem. Soc.*, 2012, **134**, 3979; (*b*) X. T. Rao, T. Song, J. K. Gao, Y. J. Cui, Y. Yang, C. D. Wu, B. L. Chen and G. D. Qian, *J. Am. Chem. Soc.*, 2013, **135**, 15559.
21. (*a*) J. Y. An, C. M. Shade, D. A. Chengelis-Czegan, S. Petoud and N. L. Rosi, *J. Am. Chem. Soc.*, 2011, **133**, 1220; (*b*) J. A. Bohrman and M. A. Carreon, *Chem. Commun.*, 2012, **48**, 5130.
22. (*a*) G. Q. Liu, D. L. Xie and C. L. Guan, *Pol. J. Chem. Technol.*, 2013, **15**, 85; (*b*) P. Sivagurunathan, K. Dharmalingam and K. Ramachandran, *J. Solution Chem.*, 2006, **35**, 1467.
23. (*a*) H. Wei, B. L. Li, Y. Du, S. J. Dong and E. Wang, *Chem. Mater.*, 2007, **19**, 2987; (*b*) H. L. Tan, B. X. Liu and Y. Chen, *Acs. Nano.*, 2012, **6**, 10505.
24. (*a*) Y. J. Cui, H. Xu, Y. F. Yue, Z. Y. Guo, J. C. Yu, Z. X. Chen, J. K. Gao, Y. Yang, G. D. Qian and B. L. Chen, *J. Am. Chem. Soc.*, 2012, **134**, 3979; (*b*) Y. Zhou, B. Yan and F. Lei, *Chem. Commun.*, 2014, **50**, 15235.

